Preparation, Photo-luminescence and Electro-Luminescence Behavior of Langmuir−Blodgett Films of Bipyridylrhenium(I) Surfactant Complexes

Vivian Wing-Wah Yam,*[a] Bin Li,[a] Yu Yang,[a] Ben Wai-Kin Chu,[a] Keith Man-Chung Wong,[a] and Kung-Kai Cheung[a]

Keywords: Luminescence / Surfactants / Langmuir−Blodgett films / Rhenium

Several bipyridylrhenium(I) surfactant complexes, *fac*-[Re(CO)$_3$(bpy)(L)]PF$_6$ [bpy = 2,2′-bipyridine, L = *trans*-4-dodecyloxy-4′-stilbazole (**L1**), *trans*-4-octadecyloxy-4′-stilbazole (**L2**), 4-(4′-dodecyloxyphenylethynyl)pyridine (**L3**)] were synthesized and characterised. The X-ray crystal structure of *fac*-[Re(CO)$_3$(bpy)(**L1**)]PF$_6$ has been determined. The complexes exhibited intense photo-luminescence which has been ascribed to the dπ(Re) → π*(bpy) metal-to-ligand charge transfer (MLCT) triplet emission. The complexes were found to form stable Langmuir–Blodgett (LB) films with relatively high collapse pressures. The organic light-emitting diodes (OLEDs) fabricated by employing the LB films of various complexes as the emitting layer exhibited electroluminescence (EL) behavior. The luminances of the EL devices were found to vary as a function of the number of LB film layers, hydrocarbon chain length and the deposition types.

Introduction

Efficient electroluminescence (EL) from organic films at low voltages was first reported in 1987.[1] Since then, a variety of EL materials have been synthesised,[1,2] and various techniques for device fabrication have been optimised.[2f,3] Recent works on the fabrication of thin-film devices for organic light-emitting diodes (OLEDs) have mainly concentrated on the use of vacuum deposition,[1,3b,4] spin coating,[5] self-assembly[3g,6,7a] and Langmuir−Blodgett (LB) techniques.[7,8] The LB film technique is interesting in that it is possible to prepare organic functional ultra-thin films with controlled thickness of a molecular size and well-defined molecular orientation.[9] In some circumstances LB films may produce films of higher quality than the general vacuum deposited or spin-coat films and may have potential applications in molecular electronic devices.[9,10]

Employment of transition metal complexes as the emissive layer in OLEDs has become one of the important subjects in recent years,[5,11] since many of them have excellent photoluminescence properties and potential advantages of achieving a maximum internal quantum efficiency of 100%.[2f] The formation efficiency of the triplet state will be triple that of the singlet state in the non-geminate pair electron combination (as in ELs), thus an improvement in the EL yield should be predicted by using triplet state materials as the emitting layer, which makes them promising candidates for OLEDs, and a number of related studies have been reported.[5,11,12] Amongst the transition metal complexes studied, those of the bipyridylruthenium(II) systems, which show ^{3}MLCT emission, have been extensively studied.[5a,5b] Other relatively less studied systems involving ^{3}MLCT emissive states include the well-known tricarbonyl(diimine)rhenium(I) complexes.[13−15]

In order to explore the potential applications of metal-based ultra-thin films in the design and construction of molecular electronic devices and to better understand the mechanism of ELs displayed by transition metal complexes in LB films, it is important to design, fabricate, and study OLEDs using LB films of metal complexes as the emissive layer. However, little attention has been devoted to this area.[8] Herein we report the synthesis of luminescent bipyridylrhenium(I) complexes with long hydrocarbon chain-containing pyridine ligands, *fac*-[Re(CO)$_3$(bpy)(L)]PF$_6$ [bpy = 2,2′-bipyridine, L = *trans*-4-dodecyloxy-4′-stilbazole (**L1**), *trans*-4-octadecyl-4′-stilbazole (**L2**), 4-(4′-dodecyloxyphenylethynyl) pyridine (**L3**); Scheme 1]. The successful preparation of stable LB films of these complexes renders their employment as the emitting layer for OLED fabrication possible and such devices have been found to exhibit electroluminescence, typical of the ^{3}MLCT emission of diiminerhenium(I) complexes. The influence of various factors on the OLEDs performance involving LB films of the complexes has also been described.

[a] Center for Carbon-Rich Molecular and Nano-Scale Metal-Based Materials Research, Department of Chemistry, and HKU-CAS Joint Laboratory on New Materials, The University of Hong Kong,
Pokfulam Road, Hong Kong
Fax: (internat.) + 852-28571586
E-mail: wwyam@hku.hk

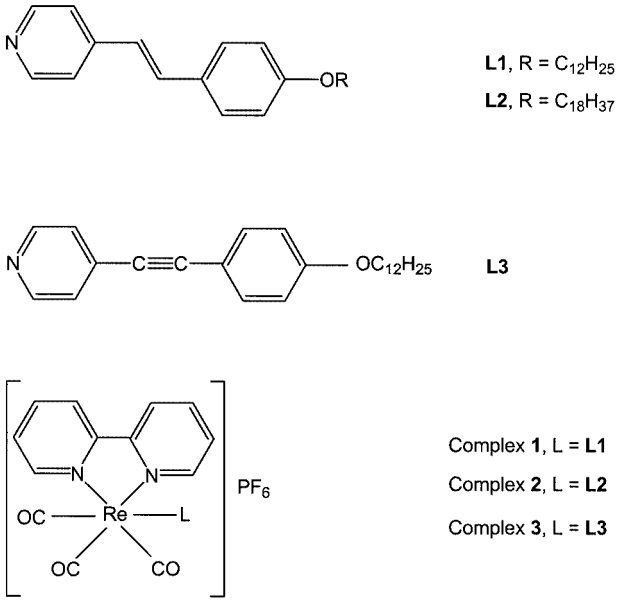

Scheme 1. Structures of ligands and corresponding surfactant Re^{I} diimine complexes

Results and Discussion

Synthesis and Characterization

The ligands **L1**,[16] **L2**,[16] **L3**[17] and the corresponding rhenium(I) complexes **1**, **2**, **3**[14e,18] were prepared according to literature methods, and their structures are shown in Scheme 1. The purity and composition of the rhenium(I) complexes were confirmed by ^{1}H NMR, IR spectroscopy, positive-ion FAB-MS and elemental analyses. The structure of **1** was determined by X-ray crystallography. The observation of three strong bands between 1900 and 2100 cm^{-1} in the infrared spectra for all rhenium(I) complexes confirms that the tricarbonyl Re^{I} moiety is in the facial arrangement.[19]

X-ray Crystal Structure

The perspective drawing of the complex cation of **1** with atomic numbering is shown in Figure 1, and selected bond lengths and angles are given in Table 1. The coordination geometry at the Re atom is distorted octahedral with the three carbonyl ligands arranged in a facial fashion. The N(1)−Re−N(2) angle of 75° is a result of the steric requirement of the bidentate diimine ligand. The C(19)−C(20) bond length of 1.342(8) Å and the bond angles of C(16)−C(19)−C(20) at 121.3(6)° and C(19)−C(20)−C(21) at 126.5(6)° are typical of the sp^2 hybridization of the styryl group. All other bond lengths and bond angles are unremarkable and are similar to those found for other related Re^{I} polypyridyl complexes.[14,19,20] The hydrophobic aliphatic chain is running along an axis that is almost perpendicular to the plane containing the Re atom and the bipyridine unit, which leads to the good LB film forming capability of the complexes.

Table 1. Selected bond lengths (Å) and angles (°) for **1**

Distances			
Re(1)−N(1)	2.171(5)	Re(1)−C(1)	1.919(7)
Re(1)−N(3)	2.230(4)	Re(1)−C(3)	1.930(8)
Re(1)−C(2)	1.941(8)	O(2)−C(2)	1.143(8)
O(1)−C(1)	1.148(7)	C(19)−C(20)	1.342(8)
O(3)−C(3)	1.145(7)	C(20)−C(21)	1.463(8)
Re(1)−N(2)	2.173(5)		
Angles			
N(1)−Re(1)−N(2)	75.0(2)	N(1)−Re(1)−C(2)	99.4(2)
N(1)−Re(1)−C(1)	95.1(2)	N(2)−Re(1)−N(3)	82.9(2)
N(1)−Re(1)−C(3)	173.8(2)	N(2)−Re(1)−C(2)	174.4(2)
N(2)−Re(1)−C(1)	93.9(3)	N(3)−Re(1)−C(1)	176.6(3)
N(2)−Re(1)−C(3)	98.8(3)	N(3)−Re(1)−C(3)	93.4(2)
N(3)−Re(1)−C(2)	96.3(2)	C(1)−Re(1)−C(3)	86.1(3)
C(1)−Re(1)−C(2)	87.0(3)	C(16)−C(19)−C(20)	121.3(6)
C(2)−Re(1)−C(3)	86.7(3)	C(19)−C(20)−C(21)	126.5(6)
N(1)−Re(1)−N(3)	85.0(2)	C(20)−C(21)−C(22)	124.6(5)

Surface Pressure−Area (π−A) Isotherms and LB Film Deposition

The π−A isotherms of the Re^{I} complexes which spread from chloroform solutions onto ultrapure water at room temperature were recorded, and are shown in Figure 2. The curves show one well-defined condensed region.

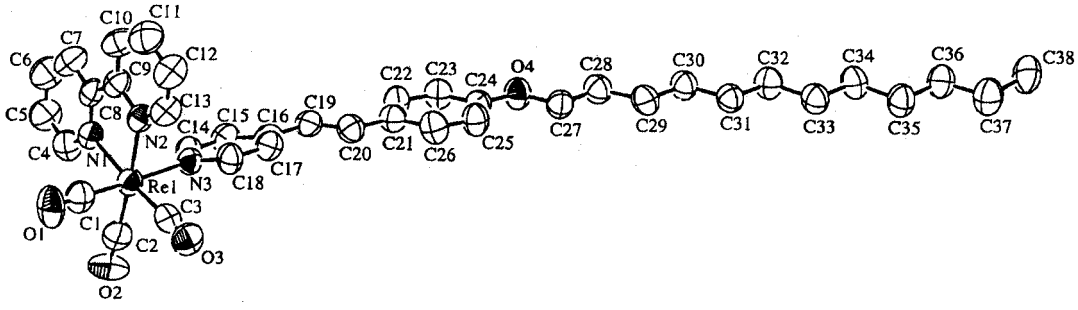

Figure 1. Perspective drawing of the complex cation of **1** with atomic numbering scheme; hydrogen atoms were omitted for clarity; the thermal ellipsoids are shown at the 50% probability level

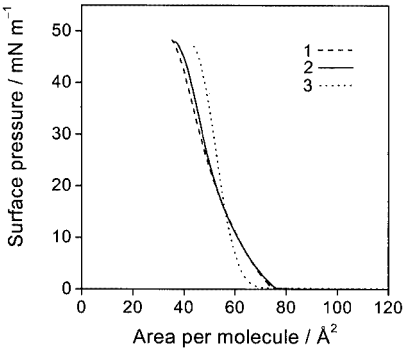

Figure 2. Surface pressure-area (π−A) isotherms of **1** (− − −), **2** (···) and **3** (---)

The molecular areas for these Re^I complexes are obtained by the extrapolation of the condensed region to zero surface pressure. The data are summarized in Table 2. It is worth noting that these complexes have similar π−A isotherms with fairly high collapse pressures as a result of the similarity in their structures.

Table 2. LB film-forming properties for complexes **1**−**3**

Complex	Molecular area (Å)^2	Collapse pressure (mN m^{-1})	Transfer ratio
1	61.5	48	0.65−1
2	60.5	49	0.80−1
3	62	48	0.65−1

The almost identical molecular areas of 61 Å^2 for these Re^I complexes match fairly well with the calculated value of 55 Å^2 based on the crystal structure of **1**. This indicates the formation of a close-packed stable monolayer at the air-water interface, probably with the long alkyl chain vertically oriented with respect to the water surface, resulting in almost no change in the area per molecule upon increasing the chain length of the hydrocarbon. Despite **1** and **3** only containing 12 -CH_2- units, their LB film-forming properties are good and similar to those of **2** which has an alkyl chain

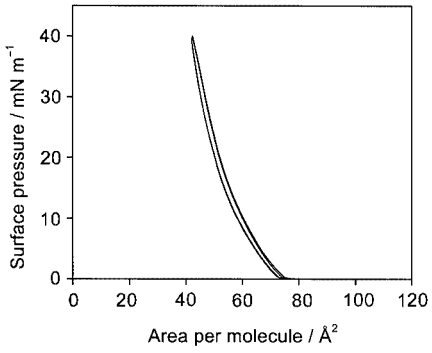

Figure 3. Compression-expanding isotherms for **1**

of 18 -CH_2- units. The formation of stable LB films with relatively short hydrocarbon chains may be advantageous in that it may minimize the resistance of the LB films in the construction of the OLED devices. The compression-expanding cycle isotherms of **1** are shown in Figure 3. No obvious hysteresis was observed, further confirming the good monolayer forming properties of the complexes.

UV/Vis Absorption Spectroscopy

The electronic absorption spectra of **1**−**3** in dichloromethane and in LB films show a high-energy absorption band at ca. 248 nm and a low-energy absorption band at ca. 364−370 nm. The high-energy absorption band is tentatively assigned as a π → π* intra-ligand transition (IL) of bipyridine. With reference to previous spectroscopic studies of the related cationic diiminerhenium(I) complexes, $[Re(CO)_3(diimine)(pyridine)]^+$,[13,14] which also exhibit a low-energy absorption band in a similar region, the low-energy absorption is ascribed to the dπ(Re) → π*(bpy) metal-to-ligand charge transfer (MLCT) transition. However, the extinction coefficients of these low-energy absorption bands in the order of 10^4 dm^3 mol^{-1} cm^{-1} in complexes **1**−**3** are much larger than those for typical MLCT transitions (approx. 10^3 dm^3 mol^{-1} cm^{-1}). In view of the similar absorption energies and extinction coefficients of the free ligands **L1**, **L2** and **L3**, the low-energy absorption band of **1**−**3** is accordingly assigned as an admixture of π → π* IL transitions of **L1**, **L2** and **L3** and dπ(Re) → π*(bpy) MLCT transitions.

Photoluminescence Properties

Complexes **1**−**3** exhibit intense greenish yellow luminescence in solution, solid state and as an LB film. The emission data for the complexes are summarized in Table 3. In general, the emission spectra of the complexes in dichloromethane and in an LB film at room temperature show broad emission bands at ca. 527−548 nm. On the basis of the previous spectroscopic assignments on the related cationic diiminerhenium(I) complexes, $[Re(CO)_3(diimine)(pyridine)]^+$,[13,14] the emission origin is assigned to be derived from the ^{3}MLCT excited state. The emission energies of the complexes in glass at 77 K were found to be blue-shifted with respect to those in solution and in LB films, and are attributed to the phenomenon of luminescence rigidochromism.[21] The emission spectra of **1** in dichloromethane and in LB films at room temperature and in EtOH/MeOH (4:1 v/v) glass at 77 K are shown in Figure 4. It is noteworthy that the luminescence quantum yield (Φ_{lum}) of **3** in fluid solution is larger than those of **1** and **2** by one order of magnitude. The lower luminescence quantum yield observed in **1** and **2** is probably due to the presence of the energy-accepting *trans*-styryl group, which would provide an additional non-radiative decay pathway for the quenching of the ^{3}MLCT excited state via an intramolecular energy transfer process, rendering the lower luminescence quantum yield. Similar observation has also been reported in the related azo- or styryl-containing rhenium(I) complexes.[15g]

Table 3. Photophysical and EL data for complex **1**−**3**

Complexes	Medium (*T*/K)	Absorption λ_{max}/nm ($\varepsilon \times 10^{-4}$/dm^3 mol^{-1}cm^{-1})	Emission λ_{em}/nm (τ_o/μs)	Luminescence quantum yield ($\Phi_{lum} \times 10^3$)	EL Luminance (cd/cm^2)[a]
1	CH_2Cl_2 (298), LB film (298), Glass[b] (77)	248 (3.38), 282 (2.12), 310 (1.83), 322 (1.80), 370 (3.91) 324, 368	539 (0.66) 527 499	6.9	6
2	CH_2Cl_2 (298), LB film (298), Glass[b] (77)	248 (3.57), 282 (2.22), 312 (1.92), 320 (2.09), 370 (3.92) 324, 366	540 (0.70) 530 492	5.7	1
3	CH_2Cl_2 (298), LB film (298), Glass[b] (77)	248 (3.29), 280 (2.12), 311 (1.98), 322 (2.56), 364 (4.44) 324, 354	548 (0.93) 546 491, 528, 555	78.0	<1

[a] ITO/LB film (25-layer)/Al. [b] EtOH/MeOH (4:1, v/v).

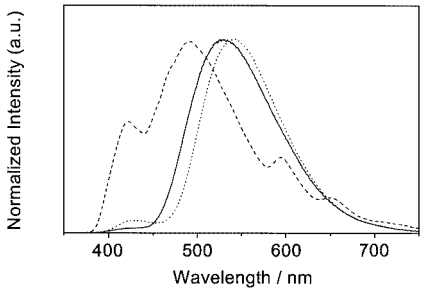

Figure 4. Normalized emission spectra of **1** (---) in EtOH/MeOH (4:1 v/v) glass at 77 K; (− − −) in 25-layer LB film; (···) in CH_2Cl_2

Electroluminescence Properties

The rhenium(I) surfactant complexes were deposited as Y-type LB films and were used as the emissive layer in single-layer OLED devices (ITO/LB film/Al; Scheme 2). An LB film thickness of at least 10 monolayers was required to prevent the possibility of a short circuit between the ITO and the aluminium electrode. Upon being forward biased with ITO at positive polarity in a continuous DC mode, the EL devices with a 25-layer LB film of **1**−**3** exhibit yellow electroluminescence (EL) with turn-on voltages of ca. 10 V. The close resemblance of the EL and PL spectra suggests that the EL of these rhenium(I) surfactant complexes involves the same excited state as PL, i.e. the triplet MLCT state or exciton. Upon forward bias, holes injected from ITO and electrons from Al migrate in the LB films and EL is generated upon recombination form excitons. The EL and PL spectra of **1** in a 25-layer LB film are shown in Figure 5.

Scheme 2. Configuration of EL cells

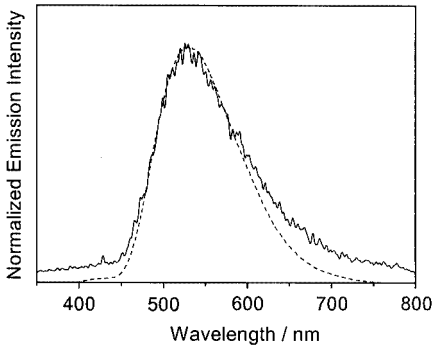

Figure 5. EL (−) and PL (···) spectra of **1** in 25-layer LB films

The EL intensity was found to vary as a function of the number of monolayers in the LB films and the relationship between the LB film layer number and the luminance of the EL devices of **1** is summarized in Table 4. The EL intensity increases with increasing layer numbers in the range of 10−20 layers, reaching a maximum at ca. 20−30 layers and then decrease upon further increase in the layer numbers of 30−40 and beyond. The EL behavior was hardly detectable for the device with an 80-layer LB film. Upon increasing the number of LB film layers, two opposite effects governing EL intensity come into effect. One is an increase in the concentration of charge carriers (both hole and electron) generated by applying DC voltage and hence an increase in the recombination probability, leading to the intensification of EL luminance. The other is an increase in the energy loss for the charge carriers passing through the LB layers, due to the larger resistance across the LB film, resulting in the diminishing of the EL intensity. For devices with 20 layers or less, it is likely that the first effect plays a more important role with such a short distance and the EL intensity is therefore increased. When the number of layers increases further (> 30 layers), the charge carrier concentration reaches a saturation level. On the other hand, fewer charge carriers can pass through the LB layers as a result of the energy loss from the long distance transporting process. Eventually, the

Table 4. Layer number-luminance relations of the EL devices of **1**

Layer number	10	20	30	40	80
Luminance (cd/cm^2)	<1	5	6	3	<1

EL intensity drops for a device with greater than 30 LB film layers. A similar phenomenon has been reported for the EL device using LB films of bis[*N*-hexadecyl-8-hydroxy-2-quinoline carboxamide]cadmium as the emitting layer.[8e,22] Optimum EL efficiency of the present EL device is obtained for the LB film in the range of 20−30 layers. It is interesting to find that complex **1**, with the shorter hydrocarbon chain, shows a higher EL intensity than **2** by a factor greater than four for the same number of LB film layers. This may be attributed to the larger energy loss for the charge carriers transporting the LB film layers with higher resistance in the longer hydrocarbon chain of **2**.

On the other hand, the EL intensity is found to depend on the deposition types of the LB films. For example, an EL device constructed of a 25-layer LB film of complex **1** in the Y-type shows an approximately 180-fold increase in EL intensity relative to that of the same device in the Z-deposition type. It is likely that the head-to-head arrangement in LB films of rhenium(I) complexes may facilitate the charge transport processes, giving rise to better EL performance (Scheme 3).[23]

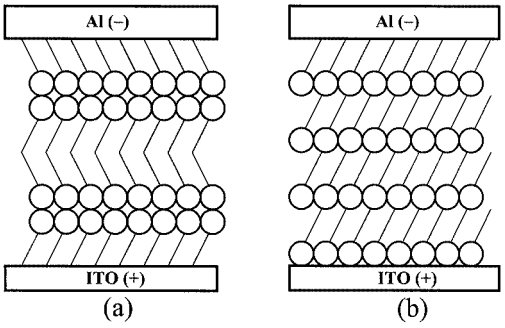

Scheme 3. Scheme of devices with different deposition types: (a) device in Y-type LB film; (b) device in Z-type LB film

In view of the poor stability of these single-layer devices, a double-layer configuration of ITO/PVK/LB film/Al was employed in order to improve the stability of the EL device. By taking advantage of the LB deposition technique which can control the deposition range, a device using the LB film of **1** was fabricated to cover only half of the area of the ITO glass. One half of the device is the ITO/PVK/Al (single-layer structure) and the other half is the ITO/PVK/**1**(LB film)/Al (double-layer structure). When the device was subjected to a forward bias using a DC power supply, the two halves of the device simultaneously emitted two different colors, a characteristic yellow EL coming from the ITO/PVK/**1**(LB film)/Al and a purple EL from the ITO/PVK/Al, typical of EL arising from PVK. In the double-layer device, PVK itself did not give rise to EL but rather acted as the hole transporting layer. The relatively even distribution of luminance indicates that uniform assemblies are formed by LB deposition on ITO/PVK. An improved performance was observed in the double-layer device. Relatively stable characteristic emission of the Re^{I} complex under the driving voltage of 7 V was observed and a maximum luminance of 9 cd/cm^2 at 18 V was achieved from the ITO/PVK/**1**(LB film)/Al device with a 25-layer LB film of **1**. The forward bias current could be obtained when the ITO electrode was positively biased and aluminium electrode negatively biased. The current increased when the forward bias voltage increased and the reverse current remained small when the ITO electrode was applied, a negative bias voltage and the Al electrode a positive bias. Figure 6 shows the current-voltage characteristics of the double-layer EL device of **1**.

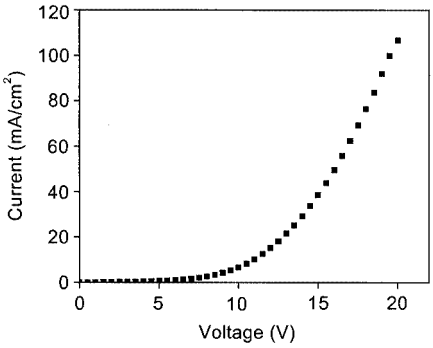

Figure 6. Current-voltage characteristics for the devices of [ITO/PVK/LB film/Al] for **1**

It is interesting to note that the luminance of the single layer device ITO/PVK/Al was 0.8 cd/m^2 when a driving voltage of 18 V was applied. Double-layer devices prepared other than using the LB technique of spin-coating of the rhenium complexes were also fabricated. The luminance of ITO/PVK:**1**/Al, ITO/PVK:**2**/Al and ITO/PVK:**3**/Al are 16, 0.7 and 0.3 cm/m^2, respectively, when the voltage applied is 18 V, similar to that obtained from LB deposition of the complexes.

Conclusions

Three Re^{I} bipyridyl surfactant complexes with hydrocarbon chain lengths of 12 and 18 were synthesised. Yellow luminescence was observed upon visible light excitation and attributed to ^{3}MLCT emission. All of them exhibit stable air-water interface behavior and are capable of forming stable multi-layer LB films on ITO substrates in an electroluminescence (EL) device. The LB films of these complexes were found to show EL behaviors with emission energies similar to those of the photo-luminescence. A decrease in the hydrocarbon chain length of the ligands in the complexes increases the EL intensity. The thickness and the deposition types of the LB films are shown to affect the luminance of the EL devices.

Experimental Section

Materials and Synthesis: 1-Bromododecane (97%, Lancaster), 1-bromooctadecane (98%, Lancaster) and $Re(CO)_5Cl$ (98%, Strem) were used as received. Piperidine (99%, Acros) was distilled over CaH_2. All other solvents for synthesis were of analytical grade and were used without further purification. The ligands **L1**,[16] **L2**,[16]

L3[17] and the corresponding rhenium(I) complexes[14e,18] were prepared according to literature methods.

The Re^{I} complexes were prepared by reaction of [Re(bpy)-$(CO)_3(CH_3CN)$]OTf with the corresponding ligand L in THF solution.[14]

***fac*-[Re(CO)$_3$(bpy)(L1)]PF$_6$ (1):** Yellow crystalline solid. Yield: 85%. Mp: 155 °C. ^{1}H NMR (300 MHz, $CDCl_3$, relative to Me_4Si): δ = 9.06 (d, *J* = 5.3 Hz, 2 H, 6,6′-H of bpy), 8.59 (d, *J* = 8.1 Hz, 2 H, 3,3′-H of bpy), 8.30 (t, *J* = 7.9 Hz, 2 H, 4,4′-H of bpy), 7.93 (d, *J* = 5.6 Hz, 2 H, pyridyl H *ortho* to N), 7.72 (d, *J* = 6.5 Hz, 2 H, 5,5′-H of bpy), 7.42 (d, *J* = 8.2 Hz, 2 H, aryl H of **L1**), 7.31 (d, *J* = 5.9 Hz, 2 H, pyridyl H *meta* to N), 7.27 (d, *J* = 15.9 Hz, 1 H, −CH=CH−), 6.86 (d, *J* = 8.1 Hz, 2 H, aryl H of **L1**), 6.71 (d, *J* = 16.1 Hz, 1 H, −CH=CH−), 3.96 (t, *J* = 6.4 Hz, 2 H, $-OCH_2-$), 1.77 (m, 2 H, $-CH_2-$), 1.44 (m, 2 H, $-CH_2-$), 1.26 [m, 16 H, $-(CH_2)_8-$], 0.87 (t, *J* = 6.2 Hz, 3 H, $-CH_3$) ppm. UV/Vis [CH_2Cl_2 λ/nm (ε × 10^{-4}/dm^{3}mol^{-1}cm^{-1})]: 248 (3.38), 282 (2.12), 310 (1.83), 322 (1.80), 370 (3.91). UV/Vis (LB film, λ/nm): 324, 368. IR (Nujol): 2028 cm^{-1} (s) ν(CO), 1927 (s) ν(CO), 1918 (s) ν(CO). Positive FAB-MS: *m*/*z* = 792 [M$^+$], 427 [M − **L1**]$^+$. $C_{38}H_{43}F_6N_3O_4PRe$ (936.9): calcd. C 48.72, H 4.59, N 4.49; found C 48.40, H 4.42, N 4.25.

***fac*-[Re(CO)$_3$(bpy)(L2)]PF$_6$ (2):** Yellow crystalline solid. Yield: 84%. Mp: 142 °C. ^{1}H NMR (300 MHz, $CDCl_3$): δ = 9.07 (d, *J* = 5.4 Hz, 2 H, 6,6′-H of bpy), 8.54 (d, *J* = 8.2 Hz, 2 H, 3,3′-H of bpy), 8.27 (d, *J* = 7.9 Hz, 2 H, 4,4′-H of bpy), 7.95 (d, *J* = 6.7 Hz, 2 H, pyridyl H *ortho* to N), 7.73 (m, 2 H, 5,5′-H of bpy), 7.41 (d, *J* = 8.8 Hz, 2 H, phenyl H of **L2**), 7.31 (d, *J* = 6.7 Hz, 2 H, pyridyl H *meta* to N), 7.25 (d, *J* = 16 Hz, 1 H, vinyl H of **L2**), 6.85 (d, *J* = 8.8 Hz, 2 H, phenyl H of **L2**), 6.70 (d, *J* = 16 Hz, 1 H, vinyl H of **L2**), 3.95 (t, *J* = 6.5 Hz, 2 H, $-OCH_2-$), 1.77 (m, 2 H, $-CH_2-$), 1.43 (m, 2 H, $-CH_2-$), 1.25 [m, 28 H, $-(CH_2)_{14}-$], 0.87 (t, *J* = 6.4 Hz, 3 H, $-CH_3$) ppm. UV/Vis [CH_2Cl_2, λ/nm (ε × 10^{-4}/dm^{3}mol^{-1}cm^{-1})]: 248 (3.57), 282 (2.22), 312 (1.92), 320 (2.09), 370 (3.92). UV/Vis (LB film, λ/nm): 366. IR (Nujol): 2028 cm^{-1} (s) ν(CO), 1929 (s) ν(CO), 1919 (s) ν(CO). Positive FAB-MS: *m*/*z* = 877 [M]$^+$, 427 [M − **L2**]$^+$. $C_{44}H_{55}F_6N_3O_4PRe$ (1021.1): calcd. C 51.76, H 5.39, N 4.12; found C 51.50, H 5.35, N 3.83.

***fac*-[Re(CO)$_3$(bpy)(L3)]PF$_6$ (3):** Yellow-orange crystalline solid. Yield: 81%. ^{1}H NMR (300 MHz, $CDCl_3$): δ = 9.05 (d, *J* = 4.6 Hz, 2 H, 6,6′-H of bpy), 8.61 (d, *J* = 8.2 Hz, 2 H, 3,3′-H of bpy), 8.32 (m, 2 H, 4,4′-H of bpy), 8.02 (d, *J* = 6.7 Hz, 2 H, pyridyl H *ortho* to N), 7.73 (m, 2 H, 5,5′-H of bpy), 7.42 (d, *J* = 8.8 Hz, 2 H, phenyl H of **L3**), 7.33 (d, *J* = 6.7 Hz, 2 H, pyridyl H *meta* to N), 6.85 (d, *J* = 8.9 Hz, 2 H, phenyl H of **L3**), 3.96 (t, *J* = 6.5 Hz, 2 H, $-OCH_2-$), 1.77 (m, 2 H, $-CH_2-$), 1.44 (m, 2 H, $-CH_2-$), 1.25 [m, 16 H, $-(CH_2)_8-$], 0.87 (t, *J* = 6.6 Hz, 3 H, $-CH_3$) ppm. UV/Vis [CH_2Cl_2, λ/nm (ε × 10^{-4}/dm^{3}mol^{-1}cm^{-1})]: 248 (3.29), 280 (2.12), 311 (1.98), 322 (2.56), 364 (4.44). UV/Vis (LB film, λ/nm): 354. IR (Nujol): 2034 cm^{-1} (s) ν(CO), 1942 (s) ν(CO), 1909 (s) ν(CO), 2185(ν), 2219 (m) ν(C≡C). Positive FAB-MS: *m*/*z* = 790 [M]$^+$, 427 [M − **L3**]$^+$. $C_{38}H_{41}F_6N_3O_4PRe$ (934.9): calcd. C 48.82, H 4.39, N 4.49; found C 48.96, H 4.34, N 4.48.

Instrumentation and Physical Characterization: The UV/Vis spectra were obtained on a Hewlett−Packard 8452A diode array spectrophotometer, IR spectra as Nujol mulls on a Bio-Rad FTS-7 spectrophotometer. ^{1}H NMR spectra were recorded on a Bruker DPX-300 NMR spectrometer with chemical shifts reported relative to tetramethylsilane. Positive-ion fast-atom bombardment (FAB) mass spectra were recorded on a Finnigan MAT95 mass spectrometer. Elemental analyses were performed on a Carlo Erba 1106 elemental analyzer at the Institute of Chemistry, Chinese Academy of Sciences. Steady-state excitation and emission spectra were obtained on a Spex Fluorolog-2 111 spectrofluorometer with or without Corning filters. Low-temperature (77 K) spectra were recorded using an optical Dewar sample holder. The OLED devices were driven at room temperature in air with a DC power supply. The EL spectra were collected on an Oriel Instruments intensified charge-coupled device (ICCD) detector (Model DH520) and were analyzed using the InstaSpec V software. The emission signal was collected by an optical fiber and dispersed onto the CCD detector with an Oriel MultiSpec 115 imaging spectrograph (Model 77480). The system was operated at −15 °C by the single-stage system in order to reduce the dark current signal. The luminance of the OLED devices was measured with a Minolta LS-110 luminance meter. The current-voltage (*I*−*V*) characteristics were studied by a Keithley 2400 autoranging sourcemeter.

X-ray Crystal Structure Determination: Crystals of **1** were obtained by slow diffusion of diethyl ether vapour into a chloroform solution of the complex. A yellow needle-shaped crystal of dimensions of 0.35 × 0.25 × 0.15 mm was used for data collection at 28 °C on a Rigaku AFC7R diffractometer with graphite monochromated Mo-K_α radiation (λ = 0.71073 Å). The space group was uniquely determined based on systematic absences and the structure was solved by direct methods (SIR92)[24a] and expanded by Fourier method and refinement by full-matrix least-squares using the software package TeXsan[24b] on a Silicon Graphics Indy computer. One crystallographic asymmetric unit consists of one formula unit. The F atoms were disordered and were placed at 12 positions with F(1) to F(12) having occupation numbers 0.87, 0.82, 0.52, 0.35, 0.64, 0.43, 0.44, 0.37, 0.49, 0.37, 0.44 and 0.26 respectively. In the least-squares refinement, 47 non-H atoms were refined anisotropically, the 12 disordered F atoms were refined isotropically, and 41 H atoms at calculated positions with thermal parameters equal to 1.3 times that of the attached C atoms were not refined. Crystal and structure determination data of **1** are collected in Table 5. CCDC-

Table 5. Crystal and structure determination data for **1**

Formula	$[C_{38}H_{41}N_3O_4Re]PF_6$
M_r (g·mol^{-1})	934.93
Crystal system	Monoclinic
Space group	$P2_1/a$ (No.14)
T, (K)	301
D_c (g cm^{-3})	1.564
V (Å^3)	3969(1)
Z	4
a (Å)	20.922(3)
b (Å)	9.104(2)
c (Å)	23.302(4)
α (deg)	90
β (deg)	116.573(2)
γ (deg)	90
F(000)	1864
Collection range	$2\theta_{max}$ = 52° (0 > *h* > 25; 0 > *k* > 11; −28 > *l* > 25)
Reflections collected	8553
Independent reflections	8321
Parameters	472
Goodness-of-fit	1.96
Final *R* indices	$R1 = 0.034$, $wR2 = 0.045$[a]
Largest difference peak/hole [e·Å^{-3}]	1.04/−0.66

[a] $w = 4\ F_o^2/\sigma^2(F_o)^2$, where $\sigma^2(F_o)2 = [\sigma^2(I) + (0.024\ F_o^2)^2]$ for 5066 reflections with $I > 3\sigma(I)$.

208904 contains the supplementary crystallographic data for this paper. These data can be obtained free of charge via www.ccdc.cam.ac.uk/conts/retrieving.html or from CCDC, 12 Union Road, Cambridge CB2 1EZ, UK [Fax: (internat.) +44-1223/336-033; E-mail: deposit@ccdc.cam.ac.uk].

LB Film Preparation and OLED Device Fabrication: Indium tin oxide (ITO) glass slides with a sheet resistance of about 30 Ω/□ were used as the positive electrode of the OLEDs. The cleaning procedure included sonication in detergent for 30 min and acetone for 30 min, rinsing in de-ionized water and isopropyl alcohol, boiling in $CHCl_3$, treatment by UV-ozone exposure, and repeated rinsing with copious amounts of ultrapure water.[25] The cleaned ITO-coated glass slides present good hydrophilic properties. The quartz substrates were cleaned by well-known standard procedures.[15j] The complexes in chloroform with concentrations of 1.00 mg cm^{-3} were spread onto a pure water sub-phase with a conductivity of 18 MΩ cm (pH, 5.6, 20 °C) using a Nima model-622 computer-controlled trough. After a 15 min. period to allow for the evaporation of chloroform, surface pressure-area (π−A) isotherms were recorded at a barrier compression speed of 150 cm^2 min^{-1}. The monolayers formed under a constant surface pressure of 25 mN m^{-1} were transferred onto hydrophilically treated substrates after maintaining the pressure constant at the transfer pressure for 10 min for stabilization, at a dipping speed of 15 mm min^{-1}. The transfer ratios of these complex films were between 0.6 and 1 (see Table 2). After the LB films were deposited, aluminium was deposited at 10^{-5} Torr to a thickness of 150 nm onto the LB film surface with a deposition rate of 1.0 nm s^{-1}. The devices ITO/[$Re(CO)_3$(bpy)(L)]PF_6/Al were obtained. The emitting area was 20 mm^2. For ITO/PVK/[$Re(CO)_3$(bpy)(L)]PF_6/Al, the [poly(9-vinylcarbazole) (PVK) layer was inserted between the LB films and the ITO electrode by spin casting solutions of PVK in $CHCl_3$ (5 mg/mL) onto the treated ITO-coated glass with a spin speed of 2400 rpm. The PVK surface is regarded as hydrophobic. The first monolayer was transferred onto a hydrophobic PVK surface on the down path. In the fabrication of double-layer devices using the spin-coating technique, the emissive layer was spin-coated onto ITO glass from a 1,1,2,2,-tetrachloroethane solution of the respective complex and PVK (10 mg:5 mg in 1 mL $C_2H_2Cl_4$) followed by deposition of aluminium by vacuum evaporation. The other procedures are the same as described above.

Acknowledgments

V. W. W. Y. acknowledges financial support from The University of Hong Kong Foundation for Educational Development and Research Limited, the Research Grants Council of the Hong Kong Special Administrative Region, China (Project No. HKU 7123/00P) and the receipt of a Croucher Senior Research Fellowship from the Croucher Foundation. B. W. K. C. and K. M. C. W. are grateful for the receipt of University Postdoctoral Fellowships, both of which are administered by The University of Hong Kong. Special thanks are due to Dr. W.-K. Chan and Miss L. S.-M Lam for their assistance in the Al electrode deposition.

[1] C. W. Tang, S. A. Vanslyke, *Appl. Phys. Lett.* **1987**, *51*, 913−915.

[2] [2a] C. W. Tang, S. A. Vanslyke, C. H. Chen, *J. Appl. Phys. Lett.* **1989**, *65*, 3610−3616. [2b] N. C. Greenham, S. C. Moratti, D. D. C. Bradley, R. H. Friend, A. B. Holmes, *Nature* **1993**, *365*, 628−630. [2c] J. Kido, C. Ohtaki, K. Hongawa, K. Okuyama, K. Nagai, *Jpn. J. Appl. Phys.* **1993**, *32*, L917−L920. [2d] C. Hosokawa, H. Higashi, H. Nakamura, T. Kusumoto, *Appl. Phys. Lett.* **1995**, *67*, 3853−3855. [2e] H. Tokuhisa, M. Era, T. Tsutsui, *Appl. Phys. Lett.* **1998**, *72*, 2639−2641. [2f] M. A. Baldo, D. F. O'Brien, Y. You, A. Shoustikov, S. Sibley, M. E. Thompson, S. R. Forrest, *Nature* **1998**, *395*, 151−154. [2g] U. Mitschke, P. Bauerle, *J. Mater. Chem.* **2000**, *10*, 1471−1507. [2h] F. G. Gao, A. J. Bard, *J. Am. Chem. Soc.* **2000**, *122*, 7426−7427. [2i] S. Lamansky, P. Djurovich, D. Murphy, F. Abdel-Razzaq, H. E. Lee, C. Adachi, P. E. Burrows, S. R. Forrest, M. E. Thompson, *J. Am. Chem. Soc.* **2001**, *123*, 4304−4312.

[3] [3a] A. Stocking, *Science* **1996**, *273*, 884−888. [3b] P. E. Burrows, V. Bulovic, G. Gu, V. Kozlov, S. R. Forrest, M. E. Thompon, *Thin Solid Films* **1998**, *331*, 101−105. [3c] T. Justel, T. H. Nikol, C. Ronda, *Angew. Chem. Int. Ed.* **1998**, *37*, 3085−3103. [3d] V. E. Choong, S. Shi, J. Curless, C. L. Shieh, H. C. Lee, J. Shen, J. Yang, *Appl. Phys. Lett.* **1999**, *75*, 172−174. [3e] G. Gu, G. Parthasarathy, P. Tian, P. E. Burrows, S. R. Forrest, *Appl. Phys. Lett.* **1999**, *86*, 4067−4075. [3f] C. J. Liang, D. Zhao, Z. R. Hong, D. X. Zhao, X. Y. Liu, W. L. Li, J. B. Peng, J. Q. Yu, C. S. Lee, S. T. Lee, *Appl. Phys. Lett.* **2000**, *76*, 67−69. [3g] J. Cui, Q. L. Huang, Q. W. Wang, T. J. Marks, *Langmuir* **2001**, *17*, 2051−2054. [3h] J. Cui, A. C. Wang, N. L. Edleman, J. Ni, P. Lee, N. R. Armstrong, T. J. Marks, *Adv. Mater.* **2001**, *13*, 1476−1480. [3i] Z. R. Hong, C. J. Liang, R. G. Li, W. L. Li, D. Zhao, D. Fan, D. Y. Wang, B. Chu, F. X. Zang, L. S. Hong, S. T. Lee, *Adv. Mater.* **2001**, *13*, 1241−1245.

[4] [4a] J. H. Burroughes, D. D. C. Bradley, A. R. Brown, R. N. Marks, K. Mackay, P. L. Burns, A. B. Holmes, *Nature* **1990**, *347*, 539−541. [4b] J. Kido, H. Hayase, K. Honogawa, K. Okuyama, K. Nagai, *Appl. Phys. Lett.* **1994**, *64*, 815−817. [4c] C. Vaterlein, H. Neureiter, W. Gebauer, B. Ziegler, M. Sokolowski, P. Bauerle, E. Umbach, *J. Appl. Phys.* **1997**, *82*, 3003−3013.

[5] [5a] F. G. Gao, A. J. Bard, *J. Am. Chem. Soc.* **2000**, *122*, 7426−7427. [5b] A. Wu, D. Yoo, J. K. Lee, M. F. Rubner, *J. Am. Chem. Soc.* **1999**, *121*, 4883−4891. [5c] V. W. W. Yam, C. L. Chan, S. W. K. Choi, K. M. C. Wong, E. C. C. Cheng, S. C. Yu, P. K. Ng, W. K. Chan, K. K. Cheung, *J. Chem. Soc., Chem. Commun.* **2000**, 53−54. [5d] Y. G. Ma, C. M. Che, H. Y. Chao, X. M. Zhou, W. H. Chan, J. C. Shen, *Adv. Mater.* **1999**, *11*, 852−857.

[6] [6a] J. K. Lee, D. Yoo, M. F. Rubner, *Chem. Mater.* **1997**, *9*, 1710−1712. [6b] M. Onoda, K. Yoshino, *Jpn. J. Appl. Phys.* **1995**, *34*, L260−L263. [6c] M. Onoda, K. Yoshino, *J. Appl. Phys.* **1995**, *78*, 4456−4462. [6d] H. Hong, D. Davidov, H. Chayet, E. Z. Faraggi, M. Tarabia, Y. Avny, R. Neumann, S. Kirstein, *Supramol. Sci.* **1997**, *4*, 67−73.

[7] [7a] E. Arias-Marin, J. C. Arnault, D. Guillon, T. Maillou, J. Le Moigne, B. Geffory, J. M. Nunzi, *Langmuir* **2000**, *16*, 4309−4318. [7b] R. Osterbacka, G. Juska, K. Arlauskas, A. J. Pal, K. M. Kalman, H. Stubb, *J. Appl. Phys.* **1998**, *84*, 3359−3363. [7c] R. Osterbacka, A. J. Pal, H. Stubb, *Thin Solid Films* **1998**, *327*, 668−670.

[8] [8a] Y. Hua, J. Peng, D. Cui, L. Li, Z. Xu, X. Xu, *Thin Solid Films* **1992**, *210*, 219−220. [8b] M. S. Weaver, D. G. Lidzey, M. A. Pavier, H. Mellor, S. L. Thope, D. D. C. Bradley, T. Richardson, T. M. Searle, C. H. Huang, H. Lui, D. Zhou, *Synth. Met.* **1996**, *76*, 91−93. [8c] A. P. Wu, T. Fujuwara, M. Jikei, M. A. Kakimoto, Y. Imai, T. Kubota, M. Iwamoto, *Thin Solid Films* **1996**, *284*, 901−903. [8d] J. M. Ouyang, L. Li, Z. H. Tai, Z. H. Lu, G. M. Wang, *Chem. Commun.* **1997**, 815−816. [8e] J. M. Ouyang, L. Li, Z. H. Tai, Z. H. Lu, G. M. Wang, *Chem. Lett.* **1997**, 199−204.

[9] F. L. Carter, " *Molecular Electronic Devices I* " Dekker, New York, **1982**.

[10] M. Schmelzer, S. Roth, C. P. Niesert, F. Effenberger, R. Li, *Thin Solid Films* **1993**, *235*, 210−214.

[11] [11a] Y. Koide, Q. W. Wang, J. Cui, D. D. Benson, T. J. Marks, *J. Am. Chem. Soc.* **2000**, *122*, 11266−11267. [11b] E. S. Handy, A. J. Pal, M. F. Rubner, *J. Am. Chem. Soc.* **1999**, *121*, 3525−3528. [11c] X. Gong, P. K. Ng, W. K. Chan, *Adv. Mater.* **1998**, *10*, 1337−1340. [11d] W. K. Chan, P. K. Ng, X. Gong, S. J. Hou, *Appl. Phys. Lett.* **1999**, *75*, 3920−3922. [11e] Y. G. Ma,

X. Zhou, J. Shen, H. Y. Chao, C. M. Che, *Appl. Phys. Lett.* **1999**, *74*, 1361−1363. [11f] J. K. Lee, D. S. Yo, E. S. Handy, M. F. Rubner, *Appl. Phys. Lett.* **1996**, *69*, 1686−1688. [11g] Y. Q. Li, Y. Wang, Y. Zhang, Y. Wu, J. C. Shen, *Synth. Met.* **1999**, 257−260.

[12] [12a] M. A. Baldo, S. Lamansky, P. E. Burrows, M. E. Thompson, S. R. Forrest, *Appl. Phys. Lett.* **1999**, *75*, 4−6. [12b] C. H. Lyons, E. D. Abbas, J. K. Lee, M. F. Rubner, *J. Am. Chem. Soc.* **1998**, *120*, 12100−12107.

[13] [13a] A. Juris, V. Balzani, F. Barigelletti, S. Campagna, P. Belser, A. V. Zelewsky, *Coord. Chem. Rev.* **1988**, *84*, 85−277. [13b] D. J. Stufkens, A. Vlcek, *Coord. Chem. Rev.* **1998**, *171*, 93−105. [13c] V. W. W. Yam, K. K. W. Lo, K. M. C. Wong, *J. Organomet. Chem.* **1999**, *578*, 3−30. [13d] M. D. Ward, F. Barigelletti, *Coord. Chem. Rev.* **2001**, *216*, 127−154.

[14] [14a] M. S. Wrighton, D. L. Morse, *J. Am. Chem. Soc.* **1974**, *96*, 998−1003. [14b] G. Sprintschnik, H. W. Sprintschnik, P. P. Kirsch, D. G. Whitten, *J. Am. Chem. Soc.* **1976**, *98*, 2337−2338. [14c] J. C. Luong, L. Nadjo, M. S. Wrighton, *J. Am. Chem. Soc.* **1978**, *100*, 5790−5795. [14d] S. M. Fredericks, J. C. Luong, M. S. Wrighton, *J. Am. Chem. Soc.* **1979**, *101*, 7415−7417. [14e] R. H. Schmehl, L. G. Whiteside, D. G. Whitten, *J. Am. Chem. Soc.* **1981**, *103*, 3761−3764. [14f] J. V. Caspar, T. J. Meter, *J. Phys. Chem.* **1983**, *87*, 952−957. [14g] P. Chen, R. Duesing, G. Tapolsky, T. J. Meyer, *J. Am. Chem. Soc.* **1989**, *111*, 8305−8306. [14h] W. M. Xue, N. Goswami, D. M. Eichhorn, P. L. Orizondo, D. P. Rillema, *Inorg. Chem.* **2000**, *39*, 4460−4467.

[15] [15a] V. W. W. Yam, V. C. Y. Lau, K. K. Cheung, *Organometallics* **1995**, *14*, 2749−2753. [15b] V. W. W. Yam, V. C. Y. Lau, K. K. Cheung, *J. Chem. Soc. Chem. Commun.* **1995**, *259*, 1195−1195. [15c] V. W. W. Yam, K. M. C. Wong, V. W. M. Lee, K. K. W. Lo, K. K. Cheung, *Organometallics* **1995**, *14*, 4043−4036. [15d] V. W. W. Yam, K. K. W. Lo, K. K. Cheung, R. Y. C. Kong, *J. Chem. Soc. Chem. Commun.* **1995**, 1191−1193. [15e] V. W. W. Yam, V. C. Y. Lau, K. K. Cheung, *Organometallics* **1996**, *15*, 1740−1744. [15f] V. W. W. Yam, K. M. C. Wong, K. K. Cheung, *Organometallics* **1997**, *16*, 1729−1734. [15g] V. W. W. Yam, V. C. Y. Lau, L. X. Wu, *J. Chem. Soc., Dalton Trans.* **1998**, 1461−1468. [15h] V. W. W. Yam, V. C. Y. Lau, K. Z. Wang, K. K. Cheung, C. H. Huang, *J. Mater. Chem.* **1998**, *8*, 89−97. [15i] V. W. W. Yam, K. Z. Wang, C. R. Wang, Y. Yang, K. K. Cheung, *Organometallics* **1998**, *17*, 2440−2446. [15j] V. W. W. Yam, Y. Yang, H. P. Yang, K. K. Cheung, *Organometallics* **1999**, *18*, 5252−5258.

[16] D. W. Bruce, D. A. Dunmur, E. Lalinde, P. M. Maitlis, P. Stying, *Liq. Cryst.* **1988**, *3*, 385−395.

[17] A. EIGhayoury, L. Douce, R. Ziessel, *Liq. Cryst.* **1996**, *21*, 143−146.

[18] G. Tapolsky, R. Duesing, T. J. Meyer, *J. Phys. Chem.* **1989**, *93*, 3885−3887.

[19] P. J. Giordano, M. S. Wrighton, *J. Am. Chem. Soc.* **1979**, *101*, 2888−2897.

[20] S. A. Moya, J. Guerrero, R. Pastene, R. Schmidt, R. Sariego, R. Sartori, J. Sanzaparicio, I. Fonseca, M. Maertiez-ripoll, *Inorg. Chem.* **1994**, *33*, 2341−2346.

[21] [21a] T. G. Kotch, A. J. Lees, *Inorg. Chem.* **1993**, *32*, 2570−2575. [21b] S. A. Moya, R. Schmidt, U. Muller, G. Frenzen, *Organometallics* **1996**, *15*, 3463−3465.

[22] G. M. Wang, C. W. Yuan, H. M. Wu, Y. Wei, *Jpn. J. Appl. Phys.* **1995**, *34*, L182−L184.

[23] G. L. Zhong, K. Z. Yang, *Langmuir* **1998**, *14*, 5502−5506.

[24] [24a] *SIR92:* A. Altomare, M. Cascarano, C. Giacovazzo, A. Guagliardi, M. C. Burla, G. Polidori, M. Camalli, *J. Appl. Cryst.* **1994**, *27*, 435−439. [24b] TeXsan: *Crystal Structure Analysis Package*; Molecular Structure Corporation. The Woodlands TX, **1985** and **1992**.

[25] M. G. Mason, L. S. Hung, C. W. Tang, S. T. Lee, K. W. Wong, W. Wang, *J. Appl. Phys.* **1999**, *86*, 1688−1692.

Received April 16, 2003
Early View Article
Published Online October 2, 2003

